Proceedings of the Combustion Institute 40 (2024) 105283

Contents lists available at ScienceDirect

Proceedings of the Combustion Institute

journal homepage: www.elsevier.com/locate/proci

# Effects of Reynolds number and ammonia fraction on combustion characteristics of premixed ammonia-hydrogen-air swirling flames

Daisuke Sato [a,b,*], Jordan Davies [a], Luca Mazzotta [a,c], Syed Mashruk [a], Agustin Valera-Medina [a], Ryoichi Kurose [b]

[a] College of Physical Sciences and Engineering, Cardiff University, Wales CF24 3AA. UK
[b] Department of Mechanical Engineering and Science, Kyoto University, Kyoto daigaku-Katsura, Nishikyo-ku, Kyoto 615-8540, Japan
[c] Sapienza University of Rome, Via Eudossiana 18, Rome 00133, Italy

ARTICLE INFO

*Keywords:*
Zero-Carbon
Turbulent flames
Reynolds number
CRN
NOx

ABSTRACT

Several studies have investigated the effects of equivalence ratio and blending ratio in constant power cases for ammonia-based fuels as ammonia is being investigated extensively as an alternative zero-carbon fuel in recent years. However, in many fields, such as power generation, it is common to operate practical equipment at constant Reynolds number (Re) conditions. To that extent, this study investigates the impact of Re ($4000 \leq Re \leq 7000$), equivalence ratio ($0.6 \leq \Phi \leq 1.45$), and ammonia volume ratio ($0.55 \leq X_{NH3} \leq 0.9$) on the combustion characteristics of $NH_3/H_2$ swirling flames. To supplement the experimental work, a previously developed Chemical Reactor Network (CRN) has been used to identify the reaction pathways affecting NOx emissions through reaction analysis. Sampled gas analysis (NO, $NO_2$, $N_2O$, $NH_3$) at the exhaust was reported for the first time at a wide range of equivalence ratios and $X_{NH3}$ at different Re. At constant Re = 6000, NO and $NO_2$ peaked at around $\Phi = 0.8 - 0.9$, while $N_2O$ became substantial at $\Phi \leq 0.8$ and unburnt ammonia became significant at $\Phi \geq 1.05$. The chemiluminescence images suggested that at Re = 6000, as $X_{NH3}$ or $\Phi$ increases, the $NH_2$* region expands, and reactions occur further downstream. Furthermore, with decreasing $X_{NH3}$ at Re = 6000 and $\Phi = 0.9$, the system becomes partially abundant in $H_2$ and H but deficient in $O_2$, suppressing the generation of O and OH radicals, and ultimately also suppressing HNO generation. This leads to the N/NH system reactions becoming dominant and increased NO consumption. NO emissions increased steadily with increasing Re at $\Phi = 0.8$, while at stoichiometry, NO emissions remained somewhat unchanged with changing Re. Findings from this study will aid further in the development of carbon-free zero-emissions systems.

## 1. Introduction

Ammonia has begun to attract attention as an energy carrier due to its high energy density and ease of transport and handling [1]. The idea of producing ammonia based on renewable energy sources such as wind and solar power, which can be produced in large quantities in certain regions of the world, and transporting it to various countries is being considered [2,3]. Because ammonia is carbon-free, burning ammonia directly as fuel could help to reduce greenhouse gas emissions, as well as the cracking cost to convert it to hydrogen. In recent years, there has been a growing body of research on ammonia combustion. However, ammonia combustion has some challenges, such as NOx emissions and unstable combustion due to its low reactivity [4].

To address these challenges, it has been proposed to use a blend of ammonia with hydrogen, another carbon-free fuel with high reactivity. Recently, research on the emissions characteristics of ammonia-hydrogen blends including NOx has been increasingly expanding. Netzer et al. [5] conducted DNS with detailed chemical kinetics for $NH_3/H_2/N_2$-air premixed flames and showed that NO formation is affected by the thermo-diffusive effects acting on the key chemical species. They also showed that the increase in local equivalence ratio due to the preferential diffusion of $H_2$ has a significant impact on NO formation. Other studies have also been conducted using swirl burners, which are commonly used in industry. Mashruk et al. [6] evaluated the unburned $NH_3$ and NOx emissions characteristics of ammonia-hydrogen blend combustion in a tangential swirl burner and confirmed that large amounts of $N_2O$ are generated under lean conditions, while large amounts of NO are generated at lean conditions approaching

* Corresponding author.
*E-mail address:* satod@cardiff.ac.uk (D. Sato).

https://doi.org/10.1016/j.proci.2024.105283
Received 4 December 2023; Accepted 31 May 2024
Available online 23 July 2024

stoichiometry. Spectroscopic analysis of the flame was also performed, and the generation of $NH_2$, NH, and OH was discussed. Kim et al. [7] conducted experimental studies using an axial swirl burner and reaction analysis using CHEMKIN-PRO and showed that the oxidation pathway from $NH_3$ to NO is different depending on the equivalence ratio. They also performed flame visualization, including the distribution of OH* and NO* radicals, and confirmed that OH promotes NO formation. Chaturvedi et al. [8] investigated the emissions using a CFD-CRN approach. They showed that NO and $N_2O$ emissions can be accurately predicted by CRN over a wide range of equivalence ratios from 0.65 to 1.2. They also constructed a quantitative reaction pathway diagram (QRPD) to identify the major NO production and consumption pathways under lean and rich combustion and found that the change in reaction pathways with equivalence ratio is dominated by OH, O, and H radicals.

In considering the practical application of this fuel blend, many of the aforementioned studies have investigated the effects of equivalence ratio and blend ratio at constant power [6,8–10]. However, in many fields, such as power generation, it is common to operate practical equipment at a constant Reynolds number [11,12]. Mashruk et al. [13] investigated the emissions characteristics of $NH_3/H_2$ flames at few constant Reynolds number cases. However, this study was restricted to the equivalence ratio of 0.65, and there are no studies that have investigated the $NH_3/H_2$ swirling flames at a wide range of equivalence ratios under constant Reynolds number.

In this study, the effects of Reynolds number, equivalence ratio, and $NH_3$vol ratio ($X_{NH3}$) on emissions characteristics for $NH_3/H_2$ swirling flames were investigated. In addition, reaction analysis using a Chemical Reactor Network (CRN) was conducted to identify the reaction pathways affecting NOx emissions.

## 2. Experimental setup and methodology

### 2.1. Tangential swirl burner

Experiments were carried out by utilizing a tangential swirl combustor ($S_g$= 1.05) as shown in Fig. 1 at atmospheric conditions (1.1 bar and 288 K). Fuel and air were injected into the premixing chamber to pass through a bluff body ($d$ = 22.5 mm) and a radial tangential swirler into the burner nozzle ($d$ = 31.5 mm). To enable optical measurements of the flame, a cylindrical GE214 quartz ($d$ = 156 mm; $h$ = 300 mm) was used to confine the swirling flames. Experiments were carried out to evaluate flame characteristics under the condition of constant bulk

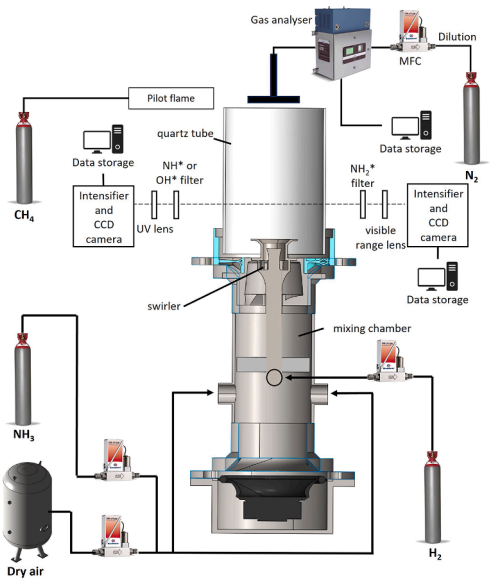


**Fig. 1.** Schematic of tangential swirl burner.

Reynolds number at the dump plane (Re= 6000) with an equivalence ratio range of $0.6 \leq \Phi \leq 1.45$, and volume fractions of ammonia in the range of $0.55 \leq X_{NH3} \leq 0.9$. Additional experiments were carried out in the ranges of $4000 \leq Re \leq 7000$, $0.6 \leq X_{NH3} \leq 0.8$, and $0.8 \leq \Phi \leq 1.2$ to evaluate the flame characteristics with changing Reynolds numbers. These condition ranges were set to avoid lean or rich blowout (LBO/RBO). Bronkhorst flow controllers were used to control the gas flow rates of ammonia, hydrogen, and air (accuracy better than ± 0.5 % within 15–95 % of the full scale), and the Reynolds number was varied by changing the volumetric flow rates of fuels and air. Flame ignition was carried out by a $CH_4$ pilot flame as shown in Fig. 1.

### 2.2. Exhaust gas analysis

The exhaust emissions (NO, $N_2O$, $NO_2$, $NH_3$, $O_2$, and $H_2O$) were measured using an Emerson CT5100 quantum cascade laser analyzer capable of measuring at 1 Hz (±1 % repeatability, 0.999 linearity). A cross-shaped probe with equispaced holes for homogeneous sample collection was placed 25 mm above the quartz exit to collect the sample gas for analysis. The sample line was heated to prevent condensation, and the measurements were performed at 463 K. $N_2$ dilution with ±10 % repeatability [13] was used for the points above the analyzer detection limits. 120 points were taken for each test condition and then time-averaged and normalized to 15 % $O_2$ (dry) condition.

### 2.3. Chemiluminescence measurements

Chemiluminescence images were captured using multiple LaVision CCD cameras simultaneously at a frequency of 10 Hz. OH* (309 nm; $A2\sum\text{+-}X2\prod$ system [14]), NH* (336 nm; $A3\prod\text{-}X2\sum$- system [14–17]), and $NH_2$* (630 nm; single peak of the $NH_2$ α band [14,18]) data were captured at selected points by utilizing various optical filters. For each test point, 200 frames were captured with LaVision Davis v10, time averaged, background corrected, and deconvolved using the Abel transformation [19] in MATLAB.

### 2.4. Chemical kinetic modelling

A previously developed chemical reactor network (CRN) [20] was employed to model selected test points in this study. Multiple perfectly stirred reactors (PSRs) were employed to model the mixing zone, flame zone, central recirculation zone (CRZ), and external recirculation zone (ERZ). The post flame zone (PFZ) was modelled as a 155 mm diameter plug flow reactor (PFR). Further details and rationale on the CRN development can be found in previous work [19]. Absolute Rate of Production (ROP) values were obtained from zero-dimensional PSR modelling of the flame field to assess the contribution of elementary reactions to NOx production and consumption. It should be noted that moderate uncertainty is associated with CRN modelling, and the system used here primarily to identify the significant reactions, rather than detailed prediction. This model employed the reaction mechanism developed by Stagni et al. [21], which has shown good performance in recent studies [13,22] for $NH_3/H_2$-air flames. There are 31 chemical species and 203 reactions in this mechanism.

## 3. Results and discussion

### 3.1. Emissions analysis at constant Re

The sampled volume fractions of NO, $N_2O$, $NH_3$, and $NO_2$ in the combustion exhaust gas for Re= 6000 are showed in Fig. 2. Mashruk et al. [13] reported that NO emissions decreased with increasing $X_{NH3}$ while keeping the Reynolds number constant at $\Phi$= 0.65. However, the results of the present study revealed that this law applies to any equivalence ratio. In addition, it was observed from this study that NO emissions decreased particularly sharply when the blend changed from

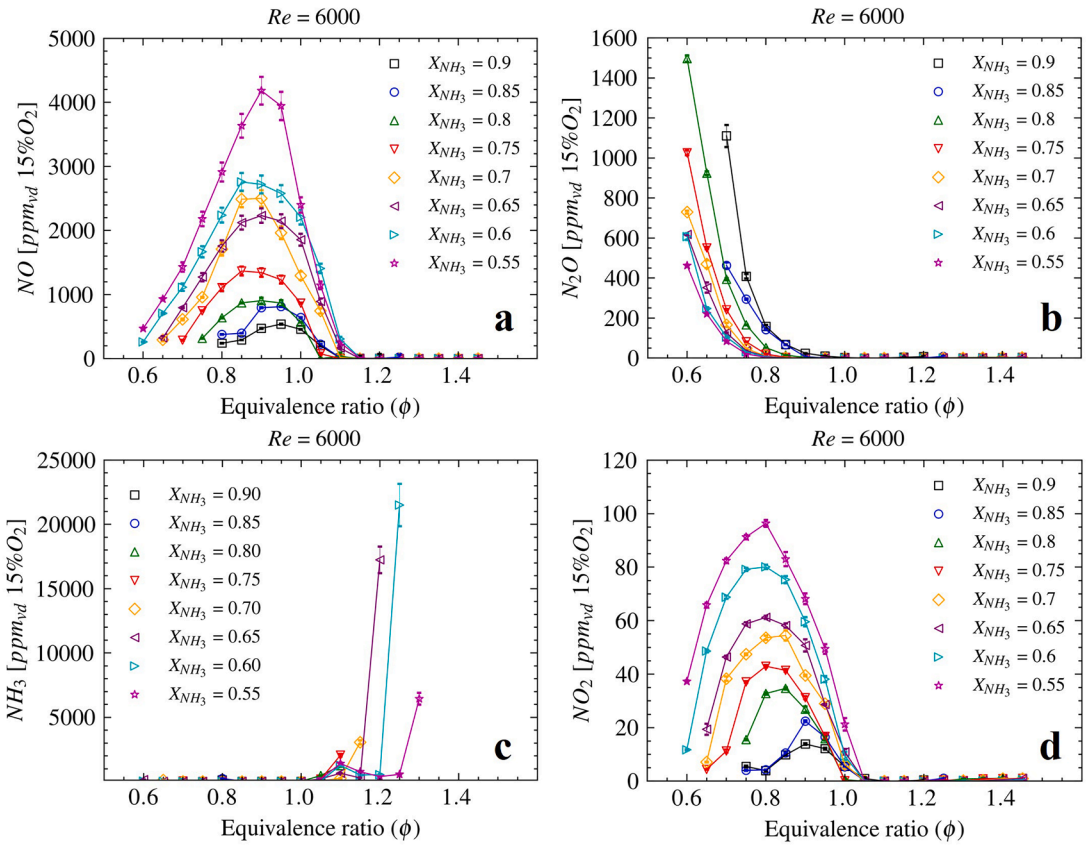


**Fig. 2.** Sampled volume fractions of NO (a), $N_2O$ (b), $NH_3$ (c), and $NO_2$ (d) at Re= 6000.

$X_{NH3}$= 0.55 to 0.6 and from 0.7 to 0.75 at around Φ= 0.9. This can be attributed to changes in volumetric gas flow rate. Under constant Re conditions, the total mass flow rate including air flow rate is constant, but since $NH_3$ has a higher density than $H_2$, as $X_{NH3}$ increases, the volumetric gas flow rate decreases. Decreasing volumetric gas flow rate reflects an increased residence time in the Flame zone and Post Flame zone, which is thought to be a contributing factor for NO reduction. However, in this measurement, as an exception, NO emissions were higher for $X_{NH3}$= 0.7 than for $X_{NH3}$= 0.65 at Φ= 0.85–0.9. This will be discussed based on chemiluminescence analysis in the next section. In addition, the peak of NO emissions was also around Φ= 0.9, as in the case of conditions with a constant power, but the peak shifted slightly towards stoichiometry for the blends with higher ammonia ratios. It was also confirmed that NO emissions are negligible for any blend at Φ= 1.15 or higher. In contrast to NO emissions, $N_2O$ emissions increased with increasing ammonia ratio at $\Phi \leq 0.9$. In addition, $N_2O$ emissions were negligible for all the blends considered here at Φ= 1.1 or higher. This has been suggested [13] to be due to the decrease in the $H_2$ concentration in the flame which resulted in decreased flame temperatures. $NH_3$ emissions were negligible at stoichiometry or lower, but emissions increased sharply as the equivalence ratio increased from Φ= 1.1 due to the decreasing availability of oxygen in the mixture. Ammonia slips increased at lower equivalence ratios for blends with high $X_{NH3}$. In addition, in this measurement, a phenomenon was confirmed in which $NH_3$ emissions increased by about 1000 ppmv around Φ= 1.1 for blends with $X_{NH3}$= 0.55–0.65. $NO_2$ emissions, like NO, tend to decrease with increasing ammonia ratio. $NO_2$ emissions were negligible for any blend at Φ= 1.05 or higher, and $NO_2$ emissions increased with decreasing equivalence ratios, with maximum measured concentrations at Φ= 0.8, and dropped thereafter. At Φ= 0.55 or lower, combustion became unstable for any blend, and the composition of the exhaust gas also became unstable.

### 3.2. *Chemiluminescence at constant Re*

The Abel-deconvoluted chemiluminescence images of OH*, NH*, and $NH_2$* at Re= 6000, Φ= 0.9, and $X_{NH3}$= 0.55, 0.7 and 0.85 are shown in Fig. 3. The colormaps of the images are normalized by the image maximum. From Fig. 3, it can be observed that the $NH_2$ region expanded as $X_{NH3}$ increased. The shape of the region also changed, with the tip of the $NH_2$* region appearing to bend in the direction of the flame central axis under low $X_{NH3}$ conditions, while the tip of the $NH_2$* region expanded radially under high $X_{NH3}$ conditions. As mentioned above,

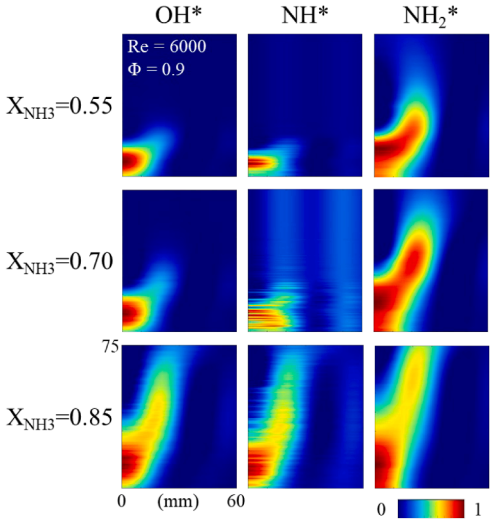


**Fig. 3.** Abel transformed OH*, NH* and $NH_2$* chemiluminescence for Re=6000 and Φ=0.9. Colourmap normalized to image maximum.

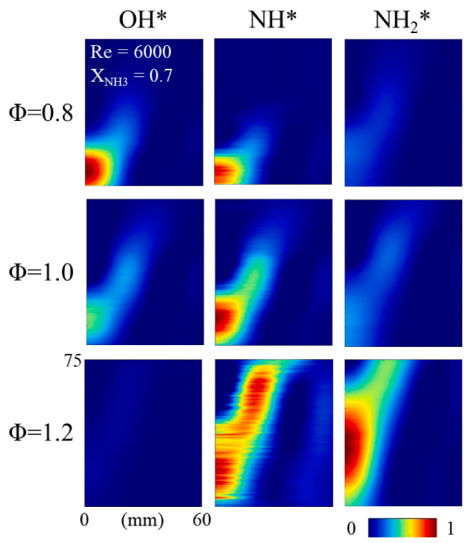


**Fig. 4.** Abel transformed OH*, NH* and $NH_2$* chemiluminescence for Re=6000 and $X_{NH3}$=0.7. Colourmap normalized to species dataset maximum.

under constant Re conditions, the volumetric gas flow rate decreases as $X_{NH3}$ increases, which could also weaken the rotation in the radial direction. However, it is considered that the change in reactivity due to the $NH_3/H_2$ blend ratio had a greater impact on the flame shape in the range of experimental conditions used in this study. In addition, as $X_{NH3}$ increased, the flame expands further away from the central axis and elongates vertically. This can be attributed to the fact that the reaction is taking place further downstream due to the decrease in reactivity and laminar flame speed caused by the increase in the ammonia ratio, also supported by the high intensity of $NH_2$* downstream under $X_{NH3}$= 0.85. This is because $NH_2$* is generated in the early stages of the oxidation reaction of $NH_3$ [23], so the region with high $NH_2$* suggests a high $NH_3$ content. Furthermore, OH* and NH* were distributed in the region close to the center of the flame and the positions are the same, but both showed a sharp decrease in intensity as $X_{NH3}$ increased. The detailed analysis of significant reactions will be discussed together with the reaction analysis results in the next section. Fig. 4 shows the Abel-deconvoluted chemiluminescence images of OH*, NH*, and $NH_2$* at Re= 6000, $X_{NH3}$= 0.7, and Φ= 0.8 – 1.2. From Fig. 4, it can be observed that the NH* intensity peaked at stoichiometry but had wider distribution at Φ= 1.2, and $NH_2$* intensity increased with increasing equivalence ratios, while OH* intensity followed the opposite trend.

### 3.3. Analysis of reactions

The absolute ROP for NO at the flame zone for Re=6000, Φ=0.9 and $X_{NH3}$=0.55, 0.7, 0.85 conditions are shown in Fig. 5. Also note that ROPs have been normalized to the maximum value in each condition for comparison purposes. First, it can be seen that $X_{NH3}$=0.55 and 0.7 show roughly similar trends for reactions related to NO. The main reaction for NO generation at the flame zone is HNO+*H*→NO+$H_2$ (R1), and the major sources of this HNO generation have been identified in previous studies [13,24] as NH+OH→HNO+*H* (R2) and $NH_2$+*O*→HNO+*H* (R3). Since the former reaction (R2) involves NH and OH, the experimental results showing higher NO emissions under conditions with stronger NH* and OH* intensity at lower ammonia fractions are also consistent. Regarding the latter reaction (R3), as $X_{NH3}$ decreases at Φ=0.9, the reaction rate increases [24]. From these findings, it is considered that lower $X_{NH3}$ leads to increased HNO generation, resulting in increased NO emissions. As with previous studies [7], the main NO consumption reaction is NH+NO→$N_2$O+*H* (R4), but interestingly, while NO generation by R1 is dominant at $X_{NH3}$=0.55, at $X_{NH3}$=0.7 and 0.85, NO consumption of R4 becomes dominant. This indicates that as $X_{NH3}$ increases,

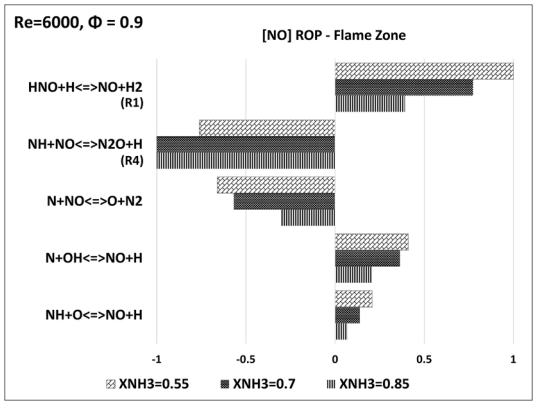


**Fig. 5.** Absolute ROP of NO at the flame zone for Re=6000, Φ =0.9 and $X_{NH3}$=0.55 to 0.85.

reactions in the N/NH system become more dominant than the HNO system. This phenomenon may be applicable to Chaturvedi's[8] theory on NO production reactions under fuel-rich conditions. That is, as $H_2$ and H derived from $NH_3$ increase in the reaction zone, the state becomes partially abundant in $H_2$ and H but deficient in $O_2$, like fuel-rich conditions, suppressing the generation of O radicals and OH radicals, and ultimately suppressing HNO generation as well. This would lead the N/NH system reactions to become dominant and increase NO consumption by reaction R4. This would also explain why the chemiluminescence intensity of OH* weakens at $X_{NH3}$=0.7 or higher and does not contradict the overall trend of decreasing NO emissions with increasing $X_{NH3}$ as shown in Fig. 2. Furthermore, Fig. 6 shows the ROP for NO at the flame zone for Re=6000, $X_{NH3}$=0.7 and Φ=0.8, 1.0, 1.2 conditions. This was calculated to see if Chaturvedi's above-mentioned theory also applied to swirling flames. Also note that ROPs indicated in Fig. 6 were normalized to the maximum value in each condition for comparison purposes. First, regarding NO production, the main reaction is R1 at Φ= 0.8 and 1.0 as H radical production can be attributed to flame temperature, but it became clear that HNO+$O_2$→NO+$HO_2$ (R5) also becomes important at Φ= 0.8 due to excess oxygen availability. Interestingly, this reaction is more than three orders of magnitude smaller under stoichiometric or fuel-rich conditions, and no previous literature or study of $NH_3/H_2$ flames has addressed this. It is also characteristic that at Φ= 1.2, the main NO production reaction is *N* + $O_2$→NO+*O* (Zeldovich, R6) rather than R1. This is a typical reaction in thermal NOx, and it can be seen that the reaction path changes when the equivalence ratio becomes stoichiometric or higher. These results show that R5 (HNO system) is important in fuel-lean conditions and R6 (N/NH system) is important in fuel-rich conditions, indicating that Chaturvedi's theory is valid even at Re=6000 constant $X_{NH3}$ cases. This notion is

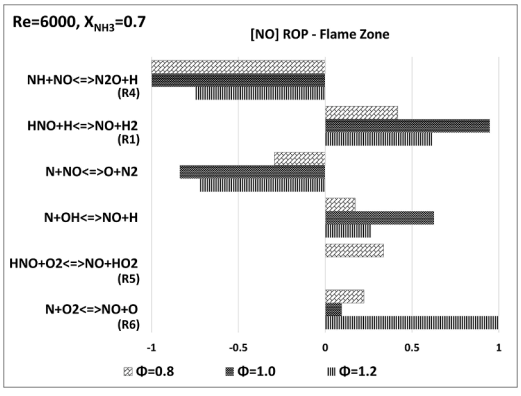


**Fig. 6.** Absolute ROP of NO at the flame zone for Re=6000, $X_{NH3}$=0.7 and Φ =0.8 to 1.2.

supported by the fact that in Fig. 4, when the fuel is lean, there is a lot of OH* related to HNO, and when the fuel is rich, there is a lot of NH* and $NH_2$*, which are the foundation of the N/NH system. In terms of NO consumption, reaction R4 is the primary reaction, as in previous studies, and it clearly outperforms R1 at Φ= 0.8 and 1.0. The data, in particular, show that this N/NH system dominance tendency at Φ=0.8 holds true even under even leaner conditions than Φ= 0.9, $X_{NH3}$= 0.7 in Fig. 5.

### 3.4. Emission analysis at changing Re

The volume fraction of NO in the combustion exhaust gas at Φ= 0.8 and 1.0 are shown in Fig. 7(a) and (b), respectively, under conditions where the Reynolds numbers were varied from 4000 to 7000. At these conditions where the Re, equivalence ratio, and $X_{NH3}$ are specified, the injection flow rates of fuel and air are automatically determined from the burner shape. Therefore, raising the Re at a constant equivalence ratio resulted in an increase in power. Although other conditions such as Φ= 1.2 and analysis of other components ($NH_3$, $NO_2$) were also carried out in this study, there were either negligible emissions data or they exceeded the analyzer's detection limit, so are omitted here. From Fig. 7, for any $X_{NH3}$ condition at Φ= 0.8, as the Re increases, NO emissions also increase. This can be attributed to the fact that with increasing Re, thermal power also increases. Mashruk et al. [13] investigated the exhaust gas characteristics at 10 kW, 15 kW, 20 kW for Φ= 0.65, confirming the tendency for NO emissions to increase with increasing thermal power. However, at stoichiometry, even when the Re was increased, the NO emissions remained almost constant, and at the $X_{NH3}$= 0.8 condition, the NO emissions sharply decreased for Re= 6000 and 7000. The reason of this phenomenon will be discussed together with the chemiluminescence measurements results in the next section. Also, as confirmed in both the above measurement results at constant Re conditions and the previous study [13], it was found that with increasing $X_{NH3}$, NO emissions had a decreasing trend at different constant Re conditions. This is due to the fact that $NH_3$-rich conditions would cause the N/NH system reactions to dominate and increase NO consumption, as well as constant Re conditions.

### 3.5. Chemiluminescence at changing Re

The Abel-deconvoluted chemiluminescence images of OH*, NH* and $NH_2$* at Φ= 0.8, 1.0 are shown in Fig. 8 and 9, respectively for Re= 5000 and 7000 at constant $X_{NH3}$= 0.6. To clarify the changes due to Re differences, the colormaps of the images are normalized to species dataset maximum. From these figures, it can be confirmed that increasing Re spreads the areas of OH*, NH* and $NH_2$* formation for both Φ= 0.8 and 1.0 conditions. This is a natural result since volumetric flow rates and

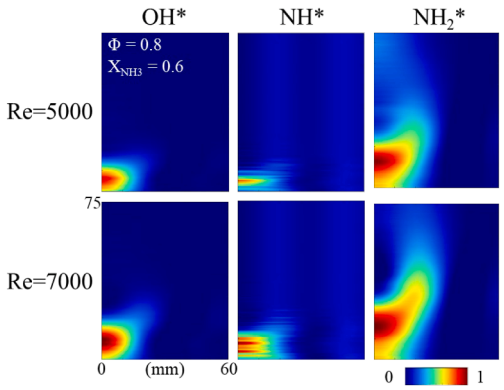


**Fig. 8.** Abel transformed OH*, NH* and $NH_2$* chemiluminescence for $X_{NH3}$=0.6 and Φ=0.8. Colourmap normalized to species dataset maximum.

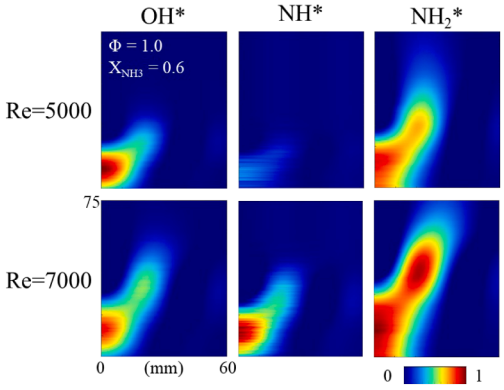


**Fig. 9.** Abel transformed OH*, NH* and $NH_2$* chemiluminescence for $X_{NH3}$=0.6 and Φ=1.0. Colourmap normalized to species dataset maximum.

power also increase with increasing Re at constant Φ. The $NH_2$* distribution also changed, and at Φ= 0.8, Re= 5000 which had the lowest volumetric flow rates, the tip of the $NH_2$* region appears to be rolled into the center of the flame. Unlike investigating by changing $X_{NH3}$ at a constant Re in Fig. 1, it can be confirmed that changes in volumetric flow rates due to changing Re directly affect flame shapes. Also, interestingly, it can be seen that increasing Re raises the intensity of NH* under both Φ= 0.8 and 1.0 conditions. This can be attributed to the enhanced circulation inside the flame due to the increasing Re, activating NH

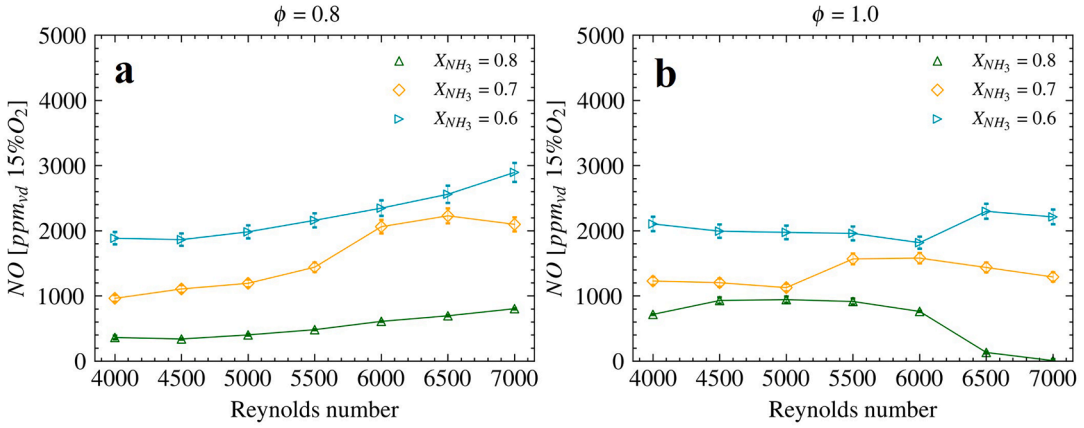


**Fig. 7.** Sampled volume fractions of NO at Φ= 0.8 and 1.0.

generation by ammonia oxidation at the flame base. Especially at stoichiometry, it can be seen that not only the intensity but also the radicals formation region expands along the flame. As discussed in the previous section using ROP analysis, the major NO consumption reaction in $NH_3/H_2$ flames up to stoichiometry is $NH + NO \rightarrow N_2O + H$ (R4). If NH, the radical responsible for this reaction, is widely supplied from the flame base due to enhanced circulation by increasing Re, it would contribute to NO consumption. In Fig. 7(b), it was expected that as Re increases, power increases and NO emissions increase, but it is presumed that NO generation and consumption are balanced by the above mechanisms, so NO emissions remain somewhat constant even when changing Re. But as an exception, NO emissions decreased at Re= 6000 and 7000 as shown in Fig. 7(b). This could be attributed to the increased circulation at high Re causing NO consumption to take over. To investigate this observation further detailed computational simulation is recommended for the future study.

## 4. Conclusions

In this study, the effects of Reynolds number, equivalence ratio, and $X_{NH3}$ on emissions characteristics for $NH_3/H_2$ swirling flames were investigated. In addition, reaction analysis using a CRN was conducted to identify the reaction pathways affecting NOx emissions.

The gas analysis revealed for the first time the exhaust emission characteristics at a wide range of equivalence ratios and $X_{NH3}$ at Re=6000. It was shown that NO emissions decrease with increasing $X_{NH3}$ while keeping the Reynolds number constant, and NOx emissions are negligible for any blend at $\Phi$= 1.15 or higher. It was also shown that $N_2O$ emissions, in contrast to NO emissions, increase with increasing $X_{NH3}$ at $\Phi \leq 0.8$.

The chemiluminescence images suggested that at Re=6000, as $X_{NH3}$ or equivalence ratios increases, the $NH_2$ region expands, and reactions occur further downstream. It was also suggested that changes in reactivity due to $NH_3/H_2$ blend ratio affect flame shape more strongly than decreases in volumetric gas flow rates due to increasing $X_{NH3}$.

The reaction analysis showed that as $X_{NH3}$ increases and $H_2$ and H derived from $NH_3$ increase in the reaction zone under constant Re conditions, the state becomes partially abundant in $H_2$ and H but deficient in $O_2$, suppressing the generation of O and OH radicals, and ultimately also suppressing HNO generation. This leads to the N/NH system reactions becoming dominant and increased NO consumption.

In addition, the effects of Reynolds number changing for exhaust emission are also investigated. And it indicates that NO emission increases with increasing Re, but this is dependent on equivalence ratios.

## Novelty and Significance Statement

The novelty of this study is based on the following reasons: this is the first study of its kind to investigate the effect of ammonia/hydrogen mixtures on exhaust gas properties in a turbulent premixed swirl flame over a wide range of equivalence ratios, ammonia fuel fraction, and Reynolds numbers, both experimentally and computationally. Specifically, combustion characteristic data were obtained for the first time under constant Reynolds number conditions at equivalence ratios other than $\Phi$= 0.65, which had previously been investigated, using gas analysis and chemiluminescence measurement. In addition to these experimental results, CRN reaction analysis was carried out in order to identify changes in the reaction pathways involved in NOx production under constant Re conditions. Although previous research has investigated the reaction pathway of $N_2O$ under constant Re number conditions, this study is the first to investigate changes in the reaction pathways involved in NO production.

## Author Contributions

- Daisuke Sato: Writing - Methodology – Figures - Data analysis - Experimental campaign.
- Jordan Davies: Data analysis - Experimental campaign.
- Luca Mazzotta: Data analysis - Figures - Experimental campaign.
- Syed Mashruk: Methodology - Experimental campaign - Review and editing – Supervision.
- Agustin Valera-Medina: Review and editing – Supervision.
- Ryoichi Kurose: Review and editing – Supervision.

## Declaration of competing interests

The authors declare that they have no known competing financial interests or personal relationships that could have appeared to influence the work reported in this paper.

## Acknowledgements

The work was supported by Project AMBURN with funding from the Department for Energy Security & Net Zero (DESNZ) under award no. IFS2–06-FLO. The experimental work was undertaken at Cardiff University's Thermofluids lab (W/0.17) with invaluable technical support from Mr. Malcolm Seaborne.

## Supplementary materials

Supplementary material associated with this article can be found, in the online version, at doi:10.1016/j.proci.2024.105283.

## References

[1] O. Elishav, et al., Progress and prospective of nitrogen-based alternative fuels, Chem. Rev. 120 (12) (2020) 5352–5436.
[2] A. Valera-Medina, et al., Review on ammonia as a potential fuel: from synthesis to economics, Energy Fuels 35 (9) (2021) 6964–7029.
[3] A. Valera-Medina, et al., Ammonia for power, Prog. Energy Combust. Sci. 69 (2018) 63–102.
[4] J. Li, et al., Study on using hydrogen and ammonia as fuels: combustion characteristics and $NO_x$formation, Int. J. Energy Res. 38 (9) (2014) 1214–1223.
[5] C. Netzer, A. Ahmed, A. Gruber, T. Løvås, Curvature effects on NO formation in wrinkled laminar ammonia/hydrogen/nitrogen-air premixed flames, Combust. Flame 232 (2021) 111520.
[6] S. Mashruk, et al., Nitrogen oxide emissions analyses in ammonia/hydrogen/air premixed swirling flames, Energy 260 (2022) 125183.
[7] J.H. Kim, et al., Combustion characteristics of premixed ammonia-hydrogen/air flames in a swirl model combustor, Int. J. Hydrogen Energy (2023) 0360–3199.
[8] S. Chaturvedi, et al., Prediction of NOx emissions and pathways in premixed ammonia-hydrogen-air combustion using CFD-CRN methodology, J. Energy Inst. 111 (2023) 101406.
[9] S. Mashruk, et al., Nitrogen Oxides as a by-product of Ammonia/Hydrogen combustion regimes, Chem. Eng.Trans. 89 (2021) 613–618.
[10] N.A. Hussein, A. Valera-Medina, A.S. Alsaegh, Ammonia- hydrogen combustion in a swirl burner with reduction of NOx emissions, Energy Procedia 158 (2019) 2305–2310.
[11] A.C. Benim, K.J. Syed, Flashback mechanisms in lean premixed gas turbine combustion, Flashback Mech. Lean Premixed Gas Turbine Combust. (2014) 1–123.
[12] A.D. Nepomnyashchiy, S.V. Suntsov, S.Y. Danilkin, V.P. Maslov, Effect of reynolds number, operating mode, turbulence parameters on profile and secondary losses of LPT, ICAS paper (2016).
[13] S. Mashruk, et al., Evolution of N2O production at lean combustion condition in NH3/H2/air premixed swirling flames, Combust. Flame 244 (2022) 112299.
[14] A. Gaydon, The Spectroscopy of Flames, Springer Science & Business Media 2012.
[15] K. Ohashi, T. Kasai, D.C. Che, K. Kuwata, Alignment dependence of the amidogen chemiluminescence in the reaction of argon(3P) atoms with the aligned ammonia molecules, J. Phys. Chem. 93 (14) (1989) 5484–5487.
[16] G.L. Schott, L.S. Blair, J.D. Morgan, Exploratory shock-wave study of thermal nitrogen trifluoride decomposition and reactions of nitrogen trifluoride and dinitrogen tetrafluoride with hydrogen, J. Phys. Chem. 77 (24) (1973) 2823–2830.
[17] T.R. Roose, R.K. Hanson, C.H. Kruger, A shock tube study of the decomposition of no in the presence of NH3, Proc. Combust. Inst. 18 (1981) 853–862.
[18] Y. Yi, et al., Plasma-Triggered CH4/NH3 coupling reaction for direct synthesis of liquid nitrogen-containing organic chemicals, ACS Omega 2 (12) (2017) 9199–9210.

[19] S. Mashruk, Nitric Oxide Formation Analysis Using Chemical Reactor Modelling and Laser Induced Fluorescence Measurements On Industrial Swirl Flames, Cardiff University, United Kingdom, 2020. PhD thesis.
[20] S. Mashruk, H. Xiao, D. Pugh, M.C. Chiong, Numerical analysis on the evolution of NH2 in ammonia/hydrogen swirling flames and detailed sensitivity analysis under elevated conditions, Combust. Sci. Technol. 195 (6) (2023) 1251–1278.
[21] A. Stagni, et al., An experimental, theoretical and kinetic-modeling study of the gas-phase oxidation of ammonia, React. Chem. Eng. 5 (4) (2020) 696–711.
[22] S.E. Zitouni, et al., Ammonia blended fuels - energy solutions for a green future, in: Proceedings of the 10th International Gas Turbine Conference, 2021.
[23] H. Xiao, A. Valera-Medina, P.J. Bowen, Modeling combustion of ammonia/hydrogen fuel blends under gas turbine conditions, Energy Fuels 31 (8) (2017) 8631–8642.
[24] Y. Sun, et al., RANS simulations on combustion and emission characteristics of a premixed NH3/H2 swirling flame with reduced chemical kinetic model, Chin. J. Aeronaut. 34 (12) (2021) 17–27.